

PLASMA DYNAMICS



## XV. PLASMA PHYSICS\*

### Academic and Research Staff

Prof. S. C. Brown  
Prof. W. P. Allis  
Prof. G. Bekefi

Prof. J. C. Ingraham  
Dr. G. Lampis  
Dr. D. R. Whitehouse

E. M. Mattison  
J. J. McCarthy  
W. J. Mulligan

### Graduate Students

M. L. Andrews  
D. L. Flannery  
E. V. George  
W. H. Glenn, Jr.

P. W. Jameson  
R. L. Kronquist  
D. T. Llewellyn-Jones  
J. E. McClintock  
J. J. Nolan, Jr.

J. C. Portinari  
G. L. Rogoff  
D. W. Swain  
F. Y-F. Tse

### RESEARCH OBJECTIVES

The aim of this group continues to be the study of the fundamental properties of plasmas. We have been placing particular emphasis on plasmas in magnetic fields, plasmas of high percentage ionization at low pressures, and, most recently, on a plasma showing turbulence in high-speed flow.

We are also studying ways of determining the characteristics of plasmas by means of very far infrared optics in the wavelength range 0.1-1 mm, and by means of optical lasers.

We continue to use more standard microwave methods, and most of our microwave techniques at the present time involve the study of microwave radiation from plasmas, with and without magnetic fields.

Theoretical work has concentrated on the study of waves in plasmas, turbulence in flowing gases, and the statistical nature of plasmas.

S. C. Brown

### A. COMPUTER PROGRAMMED "BASIC DATA OF PLASMA PHYSICS"

A project is under way, in cooperation with Project MAC, to see whether the information retrieval service of the Library TIP Program can be successfully incorporated into an attempt to revise the 1959 edition of "Basic Data of Plasma Physics" (Special Technical Report Number 2 of the Research Laboratory of Electronics, published by The Technology Press, Cambridge, Mass., and John Wiley and Sons, Inc., New York). The revision is based exclusively on bibliographical material contained in the literature of physics, programmed in the M. I. T. Technical Information Project.<sup>1</sup>

The Technical Information Project upon which this whole study is based has programmed 25 physics journals for the past few years, and, in particular, The Physical Review from the year 1959. The program contains the title, author, reference, and entire bibliography of every article. In preparing the "Basic Data" revision, the library

---

\*This work is supported by the United States Atomic Energy Commission (Contract AT (30-1)-1842).

(XV. PLASMA PHYSICS)

was searched first by subjects (such as "elastic collisions," "ion velocities," "Townsend coefficients," and so on). Whenever a key word of this sort appeared in the title of the article, the title, author, and reference was called for on the teletype console connected to the compatible time-sharing system of the MAC Project by using an IBM 7094 computer. Having turned up an entrance to a specific subject matter by searching for key words in article titles, each article thus found was subjected to a so-called "shared" bibliography search in which the computer was asked to deliver the titles of every article in the library which shared at least one bibliographic reference with the article found by title. Experience has shown that this type of machine-browsing through literature is a most efficient way of searching an entire subject-matter area. In using this system, the attempt is to create a report in open-ended form, so that anyone with access to the computer program can search the literature for material that will appear after the report is printed. As an aid for doing this, the references to individual displays of data are not given in the usual bibliographic form but in the computer-language form.

To save computer time from searching the entire library file, a subroutine called "basic data" has been specifically created in the process of putting the report together. This subroutine picks out particular journals appropriate to experimental gaseous electronics and plasma physics. This list of journals includes:

- Applied Physics Letters
- Canadian Journal of Physics
- Helvetica Physica Acta
- Indian Journal of Physics
- Japanese Journal of Applied Physics
- Journal of Applied Physics
- Journal of Chemical Physics
- Journal of the Physical Society of Japan
- Physica
- Physics Letters
- The Physics of Fluids
- Physical Review A
- Physical Review Letters
- Proceedings of the Physical Society (London)
- Soviet Physics – JETP
- Soviet Physics – Technical Physics.

Another source of data that are not always found in periodical literature is papers published in the proceedings of conferences. Some of these publications will be incorporated into the TIP Program for this specific project:

- Proceedings of the Fifth International Conference on Ionization Phenomena in Gases, held in Munich, 1961

Comptes Rendus de la VI<sup>e</sup> Conférence Internationale sur les Phénomènes d'Ionisation dans les Gaz, held in Paris, 1963

Proceedings of the Seventh International Conference on Ionization Phenomena in Gases, held in Belgrade, 1965.

This study is aimed at serving two purposes: one is to bring the book, "Basic Data of Plasma Physics," up-to-date; the other is to provide a computer method of finding new data that will appear after a report is issued. The second purpose is accomplished through the citation process, and, therefore, will be effective only if there is some article to cite. Thus if no published work has been found which supersedes the data published in "Basic Data," the previous volume's citation will be repeated with proper reference coding, so that subsequent material may be found by the computer-search method.

The citation method works because, although the TIP Program does not contain publications before 1959, the bibliographic coding is complete. If the reader so desires, he may call for the computer to present any complete bibliography or any article in the program which cites some previous article.

From the way the program has been written, it is not necessary that a cited reference to an article actually be available in the program, but only that it appear in one of the references. For example, one can ask the program to deliver all papers found in the library which cite the classic paper by Brode in the Reviews of Modern Physics, published in 1932, and in this way all papers dealing with this subject which cite Brode will be found and delivered to the searcher.

The detailed method of using the TIP Program for searching revisions for the "Basic Data" book has been worked out, and the routine searching through each item in the previous book is now in progress.

S. C. Brown

#### References

1. M. M. Kessler, *Physics Today*, March 1965, pp. 28-36.

#### B. FAR INFRARED PLASMA DIAGNOSTICS WITH A MICHELSON INTERFEROMETER

Because of ambiguities arising from sole reliance on the computer-calculated Fourier transform of the interferogram, it has become necessary to modify the previously reported<sup>1</sup> procedure for measuring phase shift and absorption of submillimeter waves in a plasma. Thus some measurements have been made with the Michelson interferometer using nearly monochromatic radiation isolated by a reflection grating. This investigation has suggested a workable procedure, in which the phase shift is measured with monochromatic radiation and absorption by using interference spectroscopy with

(XV. PLASMA PHYSICS)

the full detectable bandwidth.

The originally proposed method<sup>1</sup> of placing the plasma in one arm of the interferometer in order to measure phase shift and absorption simultaneously has proved inadequate for two reasons:

1. The spatial resolution of this method is poor,  $\sim 3$  cms, therefore radial density gradients in the plasma will tend to destroy the coherence of the two interfering beams. This gives rise to a deterioration of the fringe pattern which is indistinguishable from the reduction in fringe amplitude caused by absorption. Thus the two effects of phase shift and absorption are inseparable.

2. The method of extracting phase shifts from a computer-calculated Fourier transform leads to ambiguities when  $\phi$ , the phase shift, is greater than  $\pi/2$ , owing to the fact that the arc tangent is a multivalued function. Also, this method places a strict requirement upon the accuracy with which the zero path-difference position of the moving mirror can be relocated. This requirement can only be met by extensive rebuilding of the interferometer.

These considerations suggest the desirability of making some preliminary measurements with monochromatic radiation, thereby avoiding the use of a digital computer so that the physical effects can be observed directly. Thus the optical arrangement shown in Fig. XV-1a was used. The grating is blazed for the benefit of wavelengths close to

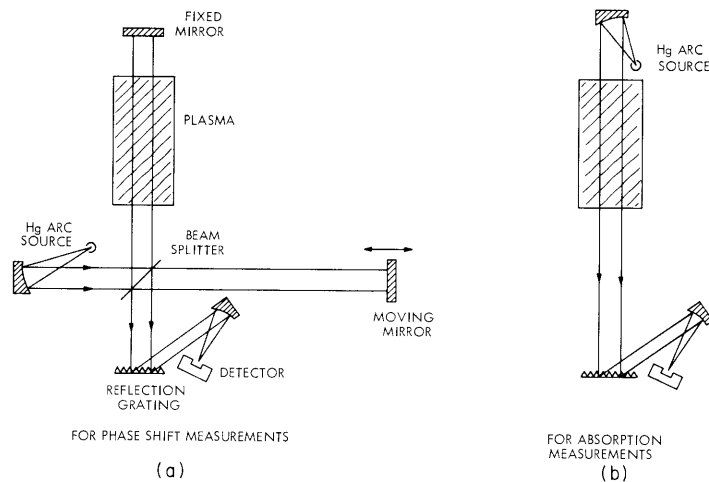


Fig. XV-1. Optical configurations.

200  $\mu$  in the first-order spectrum. The wavelength can also be measured with reasonable precision by using the Michelson interferometer in a conventional manner, and the bandwidth estimated from the number of fringes that are visible. The data presented here were obtained with a 5 per cent bandwidth centered about 205  $\mu$ .

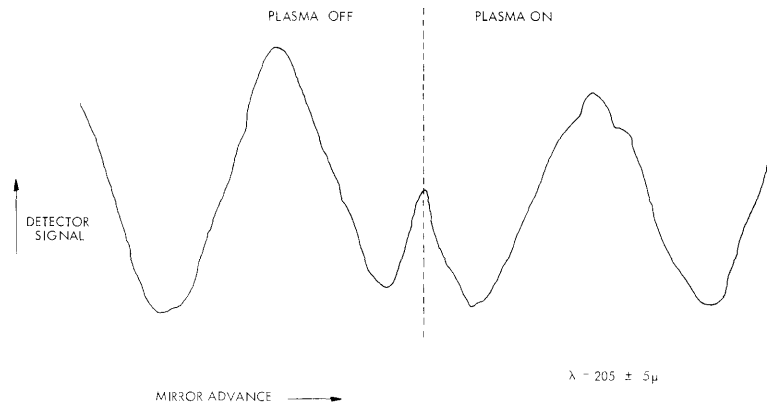


Fig. XV-2. Phase shift corresponding to  $N_e = 6.4 \times 10^{12}$  electrons  $\text{cm}^{-3}$ .

The phase shift is clearly visible in the interference pattern, which is displayed on a strip recorder, and an example is shown in Fig. XV-2. With an integration time of 3 seconds, the signal is of sufficient quality that a phase shift of approximately  $1/3$  radian, corresponding to an electron density of  $3 \times 10^{13}/L$  electrons  $\text{cm}^{-4}$ , where  $L$  is the length of the plasma column, can be detected. With a longer integration time, greater accuracy can be achieved. An upper limit to the density measurable by this method is dictated by the fact that the plasma is not uniform across the width of the infrared beam. Radial density gradients will tend to smear out the fringe pattern, and at densities greater than  $9 \times 10^{14}/L$  electrons  $\text{cm}^{-4}$  the fringes are indiscernible.

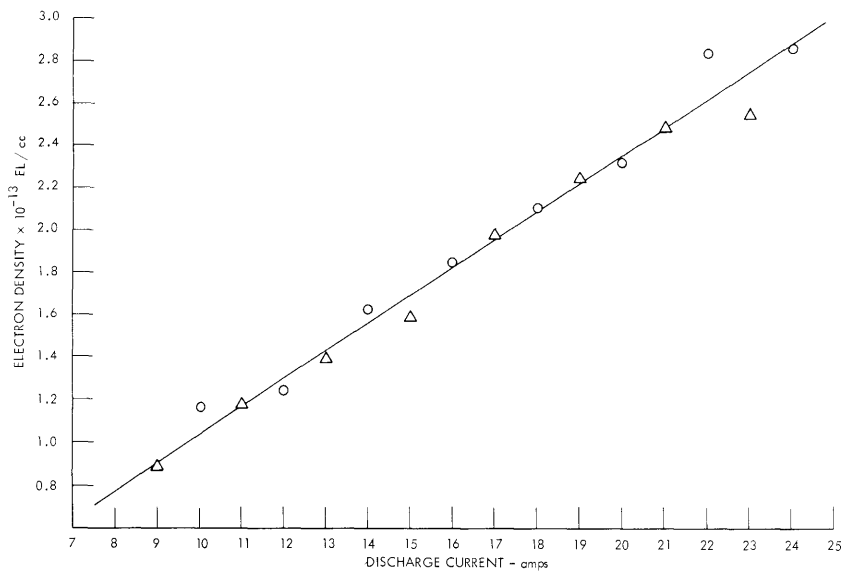


Fig. XV-3. Electron density,  $p = 1.8$  mm Hg Argon.

(XV. PLASMA PHYSICS)

The plasma used is the positive column of a DC discharge in Argon. The tube walls and the anode are water-cooled, and the cathode is a heated tungsten oxide-coated National Electric NE627 which is capable of delivering currents up to 30 amps DC. The plasma column is 30 cm long. Figure XV-3 shows the electron density as a function of discharge current at a gas pressure of 1.8 mm Hg. Note that the quality of the data decreases at densities above  $2.5 \times 10^{13}$  electrons  $\text{cm}^{-3}$  (or  $7.5 \times 10^{14}/\text{L}$  electrons  $\text{cm}^{-4}$ ), as explained above.

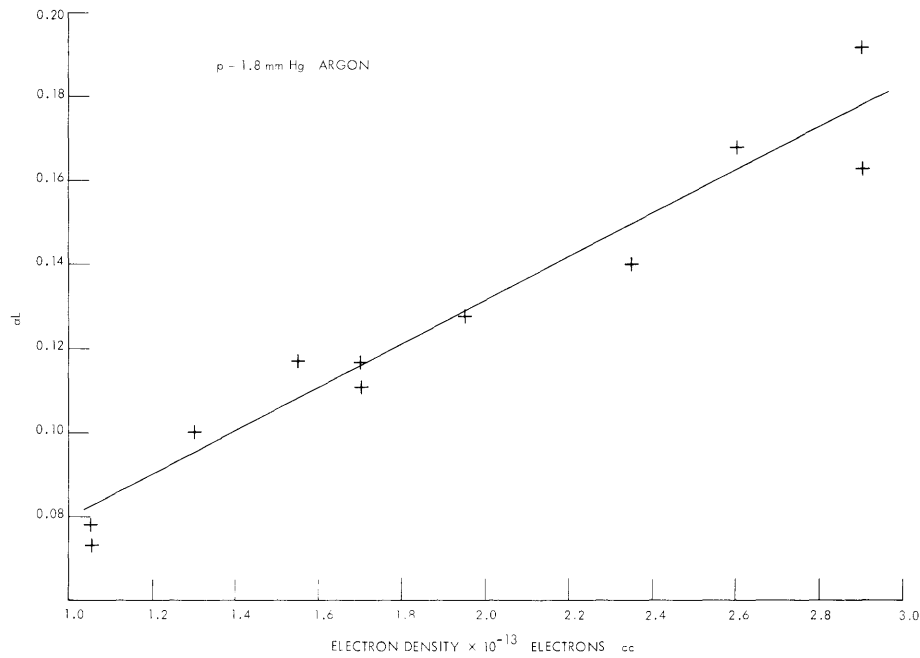


Fig. XV-4. Absorption coefficient as a function of electron density.

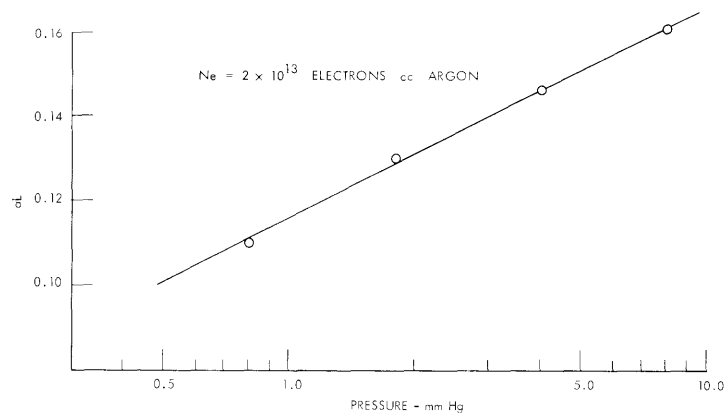


Fig. XV-5. Absorption coefficient as a function of pressure.



By using a family of curves such as the one shown in Fig. XV-3, with pressure as the parameter, it is possible to measure infrared absorption as a function of density at constant pressure, or as a function of pressure at constant density.

By using the simple optical configuration shown in Fig. XV-1b it was possible to obtain the curves shown in Figs. XV-4 and XV-5, of the absorption coefficient  $\alpha L$  as a function of density and pressure, respectively. The absorption is measured simply by comparing the transmitted signals with and without the plasma running. Figure XV-4 suggests that  $\alpha L$  is proportional to the electron density, and Fig. XV-5 suggests a logarithmic dependence upon pressure. Both of these effects are unexpected; also, the magnitude of the absorption is several orders of magnitude greater than that expected from electron-atom collision effects. It should be emphasized that the possibility that this effect is instrumental, and not due directly to the plasma, has not been eliminated beyond question.

At present, the interferometer is being mounted so that it can be placed either with the plasma in one of the two interfering beams (as in Fig. XV-1a) to measure electron density or with the plasma in the beam from the infrared source to the interferometer, so that absorption measurements can be made as a function of wavelength, by using interference spectroscopy with a digital computer. This configuration would also enable the infrared emission spectrum of the plasma to be examined by interference spectroscopy.

D. T. Llewellyn-Jones

#### References

1. D. T. Llewellyn-Jones, Quarterly Progress Report No. 71, Research Laboratory of Electronics, M.I.T., July 15, 1964, pp. 81-89.

#### C. IDEAL OPTICAL DISCRIMINATOR

In the experimental study of plasma radiation sometimes it is necessary to discriminate optically between radiation from a particular region of the plasma and that from its surroundings. This is particularly difficult when radiation from a relatively large, yet

well-defined, region of the plasma must be isolated: for example, when radiation of low intensity is being studied. Consider the case in which only radiation from a circularly cylindrical region is to be measured. Referring to Fig. XV-6, let A represent the region of interest in the experiment. Radiation from the

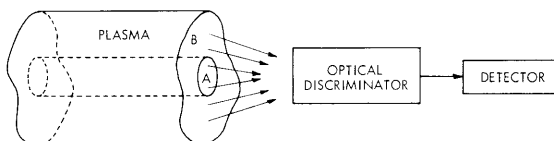


Fig. XV-6. Illustrating the function of the optical discriminator.

surrounding region, B, must be excluded from the detector. If the physical properties of the radiation from both regions are identical, the discrimination must be based on the spatial differences of the radiating regions. This report describes an optical discriminator that transmits the maximum amount of radiation from region A that is consistent with completely obstructing all radiation from region B. This problem will be considered from the point of view of geometrical optics (with diffraction effects ignored).

Ideally, all rays originating in region A reach the detector, and all those originating in B are obstructed. A ray can, however, be identified only by its direction and position in space, not by its origin; all collinear rays are equivalent in the optical system. Thus, at best, an optical discriminator would obstruct all rays that are collinear with rays from region B and transmit all rays that are definitely from region A.

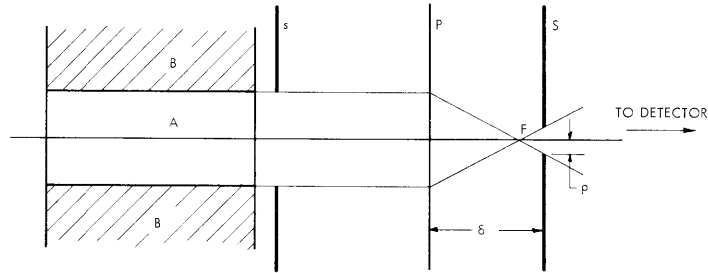


Fig. XV-7. Optical arrangement of the discriminator.

This optimum system can be achieved with the optical arrangement shown in Fig. XV-7. Region A represents the radiating cylindrical region of interest. Let A be optically thin and have a refractive index of unity. P represents the principal plane of an ideal optical system at a distance from the plasma greater than its focal length. (A single principal plane representing a "thin" optical system is used here for simplicity, although two such planes representing a more general system could be used equally well.) A three-dimensional image of the radiating plasma is formed in the space to the right of F, the focal point of the optical system. The desired discrimination between radiation from A and B is achieved by the addition of two stops, s, which has a diameter equal to that of A, and is placed as close to A as possible, and S, which has a diameter equal to that of the image of the far end of A, and is placed at the location of this image. All radiation from region B, adjacent to A, will be obstructed by these stops. If s is at the surface of the plasma, all radiation unmistakably originating in A will pass through S toward the detector.

The radius of S is

$$\rho = \left( \frac{Rf}{D - f} \right)$$

and its distance from plane P is

$$\delta = \left( \frac{Df}{D - f} \right),$$

where R is the radius of A; f, the focal length of P; and D, the distance of the far end of A from P (from the first principal plane in the more general case).

In order to understand how this discrimination occurs, consider the image of region A, which represents a source extended both laterally and axially. The nature of its image is clearly illustrated in Fig. XV-8, where the upper half of the cylindrically symmetric object A is represented by the series of arrows to the left of P and their corresponding images to the right of P. The image of A has the form of a truncated cone

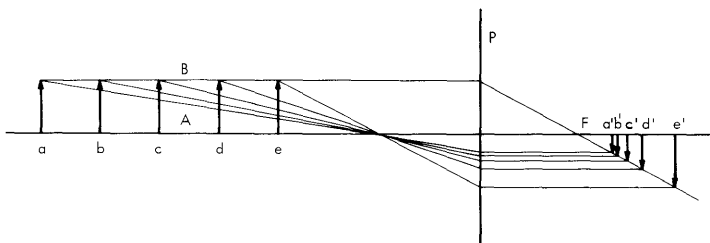


Fig. XV-8. Image formation in the optical system.

extending from  $a'$  to  $e'$ , with smaller distances between successive images for regions of A more distant from P. The edge of aperture S would lie at the head of arrow  $a'$ . Aperture s determines the boundary of the bundle of rays reaching P from any point in A or B. Aperture S determines what portion of any such bundle will reach its image point beyond S. It is sufficient to consider only rays lying in the plane of the paper and originating in A or B above the axis.

Consider the image regions  $A'$  and  $B'$  of A and B, respectively, with  $B'$  adjacent to

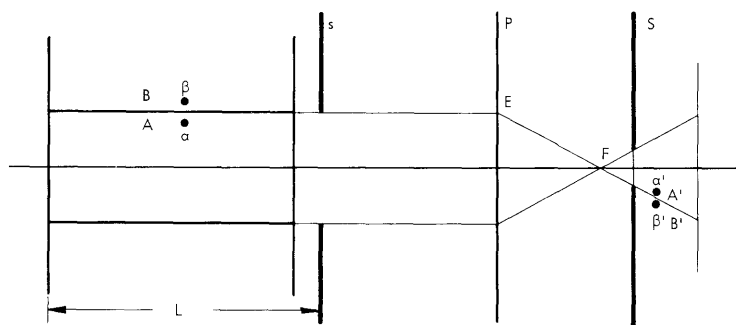


Fig. XV-9. Image regions behind the discriminator.

A'. (See Fig. XV-9.) Let  $\beta'$  be any image point in B'. The only rays that can reach  $\beta'$  through the aperture in S must intercept plane P somewhere above E. But s obstructs all such rays; thus, no rays reach B' from B.

Consider the rays approaching any image point  $\alpha'$  in A' from points in P below E. Clearly, any such rays that are collinear with rays from B will be obstructed by S, since they must pass through some points in region B', and the argument above would apply. S obstructs only those rays that are collinear with rays from B and allows all others to proceed toward their image points. For rays approaching  $\alpha'$  from above E, all those rays reaching P through B are collinear with rays from B and are obstructed by s. But if s is not directly at the front surface of the plasma, s will obstruct some rays from A that are not collinear with rays from B. The extent to which the system departs from the ideal, that is, the extent to which it obstructs rays from A that are not collinear with those from B, depends on the distance of s from the plasma surface.

From this analysis, we can determine the effective diameter,  $\Delta$ , of P corresponding to the area of P traversed by rays passing through the aperture S. This diameter is determined by the ray passing through the far upper (lower) corner of A and the lower (upper) edge of s. This ray intersects P at distance  $2R\left(\frac{D}{L} - \frac{1}{2}\right)$  from the axis. All rays passing through s and reaching P farther from the axis are collinear with rays from B, and are eliminated by S. Thus,  $\Delta = 4R\left(\frac{D}{L} - \frac{1}{2}\right)$ , where L is the distance of the far end of A from s.

Note that this discriminator obstructs any radiation reflected from the inner surface of region B. This might be significant, for example, if region B represents the walls of a discharge tube.

#### 1. Comparison of the Optical Discriminator with the Ordinary Collimator

It is worth while to compare this optical discriminator with an alternative system such as an ordinary collimator, which consists essentially of a lens with a small aperture centered at its focal point. Such a system is primarily a directional discriminator, transmitting only those rays that enter at an angle with respect to the axis which is less than some characteristic angle. Ideally, with an infinitesimal aperture at its focal point, only rays parallel to the axis are transmitted; but with a finite aperture, the radiation transmitted from a given plasma volume element is that contained in a particular cone directed parallel to the axis. This cone is the same for all radiating volume elements. The collimator transmits radiation only from certain spatial regions solely because of its finite transverse dimensions.

In an ordinary collimator the solid angle of the accepted radiation cone is determined by the size of the aperture centered at the focal point. The region of space from which radiation is accepted is determined by the effective aperture of the system, which is given by the dimensions of either the optical components or an aperture between the

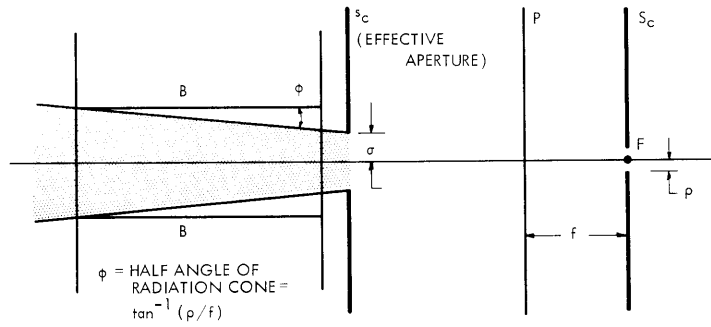


Fig. XV-10. Ordinary collimator.

optical components and the radiator (see Fig. XV-10). Clearly, for any point in the radiator only that portion of the light contained in the relevant cone intercepting the effective aperture will be transmitted through the system.

Such a collimator will transmit no radiation from B if no part of B is contained in its acceptance space (shaded region in Fig. XV-10). This collimator certainly cannot transmit as much radiation from region A as the discriminator already described, since the discriminator can transmit the maximum possible amount from every volume element of A, while the collimator accepts no radiation from some regions of A. The collimator, in a sense, operates on every radiating volume element identically, whereas the optical discriminator operates on each volume element individually, accepting from each the maximum amount of radiation consistent with discriminating against all unwanted radiation. Nevertheless, it is worth comparing the total amount of transmitted radiation in the two cases to see if the advantages of the optical discriminator warrant its use.

In this comparison let region A be a homogeneous, isotropic radiator with negligible absorption. For any radiating volume element the amount of radiation transmitted is

$$I\left(\frac{\Omega}{4\pi}\right) dv,$$

where  $I$  is the total radiation per unit volume emitted equally in all directions,  $dv$  is the volume element, and  $\Omega$  is the solid angle transmitted by the optical system. The total amount of radiation transmitted is

$$\frac{I}{4\pi} \int_A \Omega dv = \frac{I}{4\pi} W,$$

where  $W$  is the geometrical factor that we shall calculate for both discriminator and collimator.

#### a. Optical Discriminator

At any point  $p$  in A (see Fig. XV-11)  $\Omega$  is the solid angle subtended by the overlap of the circular area of aperture  $s$  with the projection in the plane of  $s$  of the far end of A

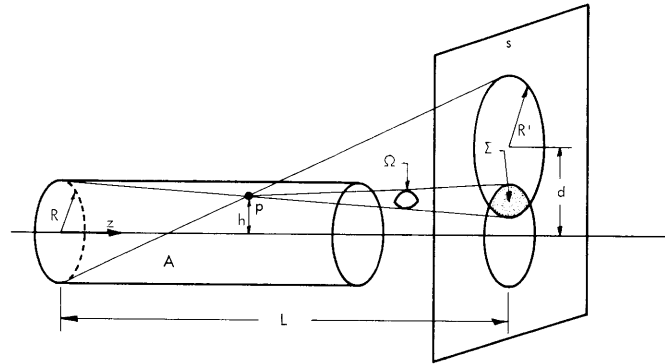


Fig. XV-11. Solid angle transmitted by the discriminator.

(originally the same size as s) through the point p. This solid angle contains all rays from p that are not collinear with rays from B, and pass through s, however far s is from the plasma.

If R is the radius of s or A, and R' is the radius of the projection on s, then  $R' = \left(\frac{L-z}{z}\right)R$ , where z is the axial position of p measured from the far end of A, and d is the distance between the center of s and the center of the projected circle. Thus

$$d = \left(\frac{hL}{z}\right),$$

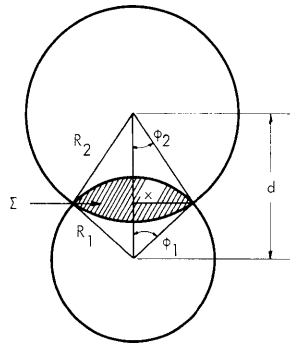


Fig. XV-12. Overlap area for two circles.

where h is the distance of p from the axis.

Since an exact calculation of  $\Omega$  is quite difficult, we will make the assumption that the distance  $(L-z)$  between p and s is large compared with the dimensions of the shaded area, and we approximate

$$\Omega \approx \frac{(\text{shaded area})}{(L-z)^2} \approx \frac{\Sigma}{(L-z)^2}.$$

Now, for any two circles of radii  $R_1$  and  $R_2$ , where  $R_2 \geq R_1$ , the overlap area  $\Sigma$  (see Fig. XV-12) is given by

$$\Sigma = R_1^2 \phi_1 + R_2^2 \phi_2 - xd, \quad d > (R_2 - R_1)$$

$$\Sigma = \pi R_1^2, \quad d < (R_2 - R_1).$$

The second equation represents the smaller circle as being completely contained within the larger. These equations can also be written

$$\Sigma = R_1^2 \cos^{-1} \left[ \frac{d^2 + R_1^2 - R_2^2}{2dR_1} \right] + R_2^2 \cos^{-1} \left[ \frac{d^2 + R_2^2 - R_1^2}{2dR_2} \right] - \frac{1}{2} \sqrt{4d^2 R_1^2 - (d^2 + R_1^2 - R_2^2)^2}, \quad d > (R_2 - R_1) \quad (1)$$

$$\Sigma = \pi R_1^2, \quad d < (R_2 - R_1).$$

For the discriminator we have two circles of radii  $R$  and  $\left(\frac{L-z}{z}\right)R$  with  $d = (hL/z)$ . Substituting these values in Eq. 1 yields

$$\Sigma = R^2 \cos^{-1} \left[ \frac{\left(\frac{L}{z}\right)^2 \left(\frac{h}{R}\right)^2 + 1 - \left(\frac{L}{z} - 1\right)^2}{2\left(\frac{L}{z}\right)\left(\frac{h}{R}\right)} \right] + \left(\frac{L}{z} - 1\right)^2 R^2 \cos^{-1} \left[ \frac{\left(\frac{L}{z}\right)^2 \left(\frac{h}{R}\right)^2 + \left(\frac{L}{z} - 1\right)^2 - 1}{2\left(\frac{L}{z}\right)\left(\frac{h}{R}\right)\left(\frac{L}{z} - 1\right)} \right] - \frac{R^2}{2} \sqrt{4\left(\frac{L}{z}\right)^2 \left(\frac{h}{R}\right)^2 - \left[\left(\frac{L}{z}\right)^2 \left(\frac{h}{R}\right)^2 + 1 - \left(\frac{L}{z} - 1\right)^2\right]^2}. \quad (2)$$

It is convenient to normalize  $\Sigma$  to the cross-section area of A. A plot of  $(\Sigma/\pi R^2)$  vs  $(h/r)$  for various positions along A (see Fig. XV-13) shows that  $\Sigma(h/R)$  may be approximated by a linear function in the regions where  $\Sigma$  decreases with  $(h/R)$ . If we do this and integrate over the volume of A, we get

$$W = \left(\frac{\pi^2 R^4}{L}\right) \left\{ \frac{4}{3} \left(\frac{\ell}{L}\right) + \frac{1}{3(1-\ell/L)} + \frac{2}{3} \ln \left(1 - \frac{\ell}{L}\right) - \frac{1}{3} \right\}, \quad \ell < \frac{L}{2} \quad (3)$$

$$W = \left(\frac{\pi^2 R^4}{L}\right) \left\{ \frac{4}{3} \left(\frac{\ell}{L}\right) - \frac{1}{3} \left(\frac{L}{\ell}\right) - \frac{2}{3} \ln \left(\frac{\ell}{L}\right) + 1 - \frac{4}{3} \ln 2 \right\}, \quad \ell > \frac{L}{2}, \quad (4)$$

where  $\ell$  indicates the limit of integration along the axis;  $\ell$  can be the length of the plasma if the plasma does not extend to  $s$ .

#### b. Ordinary Collimator

The radiation transmitted by an ordinary collimator can be calculated in a similar manner. In this case at any point  $p$  in A,  $\Omega$  is the solid angle subtended by the overlap of the circular area of the effective aperture  $s_c$  with the circular cross section of the cone from  $p$  (of half-angle  $\phi$ ), the axis of this cone being parallel to the system axis.

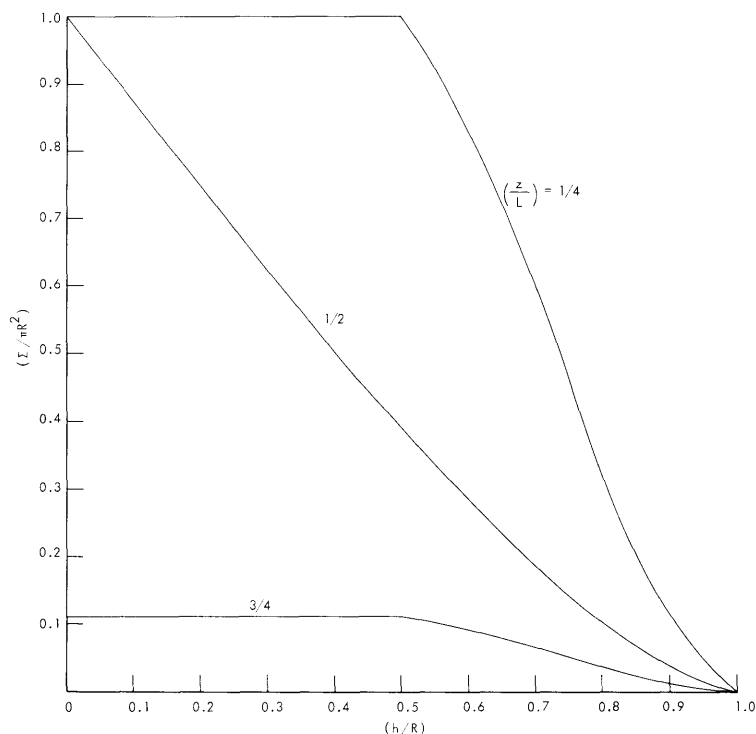


Fig. XV-13. Plot of  $(\Sigma/\pi R^2)$  vs  $(h/R)$  for various positions along the plasma.

All rays from  $p$  contained in this solid angle are transmitted by the collimator.

Again, we make the approximation that the distance between  $p$  and the aperture is much greater than the dimensions of the overlap area  $\Sigma$ . Following a procedure similar to that for the discriminator, we get

$$W = \left( \frac{\pi^2 R^4}{L} \right) \left\{ \frac{1}{3} \left( \frac{\sigma}{R} \right)^4 \left( \frac{\ell/L}{1 - \ell/L} \right) + \left( 1 - \frac{\sigma}{R} \right)^2 \left( \frac{\sigma}{R} \right)^2 \left( \frac{\ell}{L} \right) \right\}, \quad \ell < \ell_0, \quad \ell_0 > 0 \quad (5)$$

$$W = \left( \frac{\pi^2 R^4}{L} \right) \left\{ \frac{4}{9} \left( \frac{\sigma}{R} \right)^3 - \frac{7}{9} \left( \frac{\sigma}{R} \right)^4 + \left( 1 - \frac{\sigma}{R} \right)^2 \left( \frac{\sigma}{R} \right)^2 \left( \frac{\ell}{L} \right) - \frac{1}{9} \left( 1 - \frac{\sigma}{R} \right)^4 \left( 1 - \frac{\ell}{L} \right)^3 \right\}, \quad \ell > \ell_0, \quad \ell_0 > 0 \quad (6)$$

$$W = \left( \frac{\pi^2 R^4}{L} \right) \left\{ \frac{1}{9} \left( 1 - \frac{\sigma}{R} \right)^4 + \left( 1 - \frac{\sigma}{R} \right)^2 \left( \frac{\sigma}{R} \right)^2 \left( \frac{\ell}{L} \right) - \frac{1}{9} \left( 1 - \frac{\sigma}{R} \right)^4 \left( 1 - \frac{\ell}{L} \right)^3 \right\}, \quad \ell_0 < 0, \quad (7)$$

where  $\ell_0 = \frac{\left[ 1 - 2 \left( \frac{\sigma}{R} \right) \right]}{\left[ 1 - \left( \frac{\sigma}{R} \right) \right]} L$ , with  $\sigma$  the radius of the effective aperture  $s_c$ .



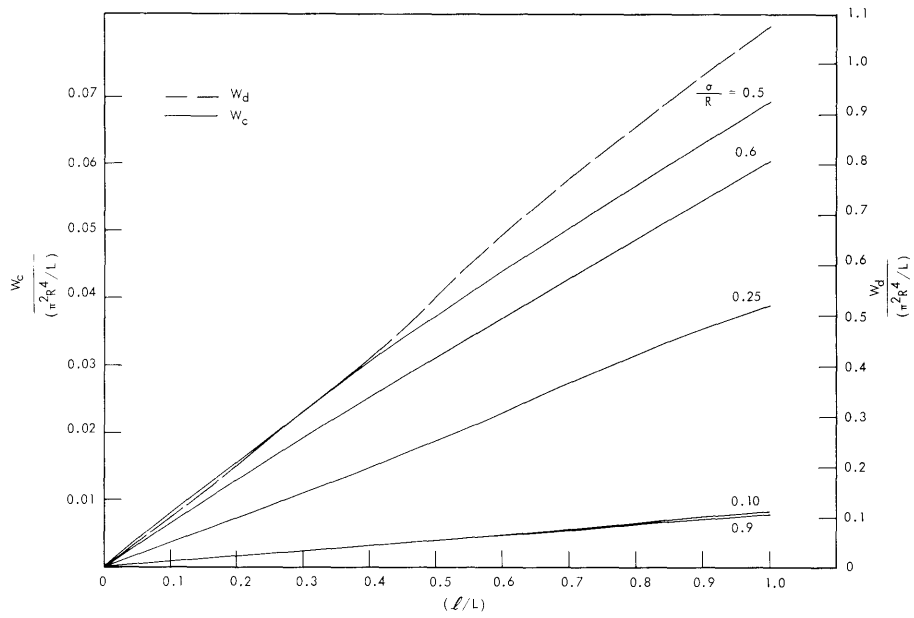


Fig. XV-14. Plot of  $[W/(\pi^2 R^4/L)]$  vs  $(\ell/L)$  for discriminator ( $W_d$ ) and collimator ( $W_c$ ).

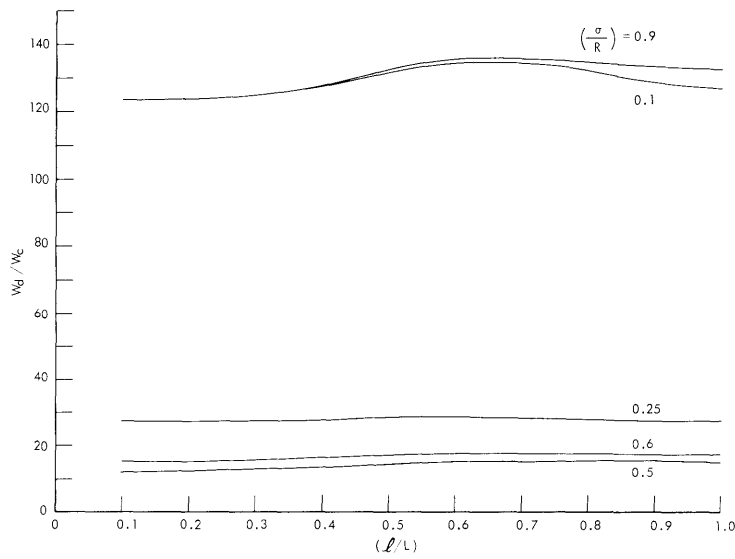


Fig. XV-15. Plot of  $(W_d/W_c)$  vs  $(\ell/L)$  for various collimator aperture sizes.

In Fig. XV-14,  $W$  is plotted as a function of  $(\ell/L)$  both for the discriminator ( $W_d$ ) and the collimator ( $W_c$ ). Here,  $W$  is normalized to  $(\pi^2 R^4/L)$ , where the value of  $L$  is taken to be the same for both cases. In either case the aperture  $s$  should be as close to the plasma as possible, and this position would depend only on the physical experimental arrangement. Note that if the acceptance space of the collimator is made to border on the outer edge of the far end of region A and the position of aperture  $s_c$  is fixed, then the size of the radiation acceptance cone is inversely related to the aperture radius  $\sigma$ .

The transmission of the discriminator is significantly greater than that of the collimator. This is shown even more clearly in Fig. XV-15, where  $(W_d/W_c)$  is plotted as a function of  $(\ell/L)$  for various collimator aperture sizes.

Although this comparison refers specifically to a homogeneous, isotropic radiator, the discriminator will transmit more radiation than the collimator for any radiator not so restricted.

## 2. Aberrations

Any real optical system will exhibit aberrations to some degree, and their effect on the operation of the discriminator must be determined. Aberrations are important only to the extent that they require alterations from the ideal optical arrangement in order that all light from B will be eliminated while as much light as possible from A will be transmitted. The quality of the image A' is not of primary concern. Consequently, a consideration of aberrations in terms of the usual specific image defects (i. e., astigmatism, coma, spherical aberration, etc.) is not the most constructive approach here. Rather, for any given real situation, the problem is to determine what ray from B intersects the plane of S closest to the axis. Adjusting the aperture S to obstruct this ray will correct for aberrations.

This correction must be determined for the particular system that is being used. In some cases it is possible to do this experimentally by arranging for only region B to radiate and closing down the aperture S until radiation is no longer detected (e. g., if region B represents discharge tube walls, these walls may be heated with no plasma inside). Clearly, the effects of misalignments, irregularities of optical components, refraction in windows, and so forth must also be examined for particular experimental systems.

G. L. Rogoff